2025 IEEE 64th Conference on Decision and Control (CDC)
December 10-12, 2025. Rio de Janeiro, Brazil

Efficient Configuration-Constrained Tube MPC via Variables Restriction and Template Selection

Filippo Badalamenti, Sampath Kumar Mulagaleti, Mario Eduardo Villanueva, Boris Houska, Alberto Bemporad

Abstract— **Configuration-Constrained Tube Model Predictive Control (CCTMPC) offers flexibility through polytopic parameterization of invariant sets and optimization of an associated vertex control law. However, this flexibility introduces a trade-off between set accuracy and computational complexity. This paper addresses it with two contributions. First, a structured framework is proposed that restricts optimization degrees of freedom in a systematic way, significantly reducing online computation while retaining stability guarantees. This framework aligns with Homothetic Tube MPC (HTMPC) under maximal constraints. Second, a template refinement algorithm is introduced, which iteratively solves quadratic programs to balance polytope complexity and conservatism. Simulations on an illustrative benchmark and a high-dimensional ten-state system demonstrate the contributions' efficiency, achieving robust performance with minimal computational overhead. The results validate a practical pathway to exploit CCTMPC's adaptability without compromising real-time viability.**

I. Introduction

Tube Model Predictive Control (TMPC) has established itself as a key tool in robust control, thanks to its ability to enclose all state realizations of an uncertain system within a sequence of bounded sets [1]–[3]. Among the various parameterizations, polytopic ones are particularly appealing, as they enable the online solution of a Quadratic Programming (QP) problem [4]. Prominent examples include Rigid [5], [6], Homothetic [7], and Elastic [8], [9] Tube MPC schemes. These typically enforce set invariance via linear feedback laws, though formulations with freely parameterized control laws have also been explored [10].

Configuration-Constrained Tube MPC (CCTMPC) [11] introduces a different paradigm based on polytopic sets with fixed facet orientations, referred to as the *template*. In this framework, all polytopes share the same combinatorial structure, meaning each vertex is defined by the intersection of a fixed set of hyperplanes. This structural consistency allows facet displacements to be optimized online within bounds that preserve the configuration, while maintaining a linear relationship between facet displacements and vertex positions. Consequently, both the set geometry and the associated vertex control law [12] can be optimized online, inherently supporting systems with multiplicative uncertainty.

F. Badalamenti (Corresponding Author, filippo.badalamenti@imtlucca.it), S.K. Mulagaleti, M.E. Villanueva and A. Bemporad are with IMT School for Advanced Studies Lucca, Piazza San Francesco 19, 55100, Italy. B. Houska is with ShanghaiTech University, China. This work has received support from the European Research Council (ERC), Advanced Research Grant COMPACT (Grant Agreement No. 101141351)

Despite its advantages, CCTMPC poses two main challenges: First, joint optimization of geometry and control leads to high-dimensional problems, especially for large-scale systems. Second, performance and computational efficiency depend not only on the number but also on the orientation of template hyperplanes, making the trade-off between expressiveness and tractability critical.

Contribution: This paper addresses these challenges through two complementary innovations: First, a family of Tube MPC controllers that reduce the number of optimization variables in a systematic way, spanning from full CCTMPC flexibility to a highly efficient formulation reminiscent of Homothetic Tube MPC (HTMPC). Second, an iterative template refinement algorithm that incrementally enriches polytope structure via QPs, allowing users to tune the trade-off between conservatism and complexity.

Outline: The paper is structured as follows: Section II formalizes the problem and introduces the necessary mathematical framework. Section III presents the proposed controller family, discussing its theoretical properties. Section IV details the template refinement procedure. Section V reports numerical results, including a 10-state quadcopter model. Section VI summarizes the contributions and outlines directions for future research.

Notation: $\mathbb{I}_n$ denotes the $n \times n$ identity matrix. A block-diagonal matrix composed of $Q_1,...,Q_n$ is written as $\mathrm{blkd}(Q_1,...,Q_n)$. The operator convh denotes the convex hull, and $\|z\|_Q^2 := z^\top Q z$. For compact sets $\mathcal{A} \subseteq \mathcal{B} \subset \mathbb{R}^n$, $\mathrm{d}_{\mathcal{B}}(\mathcal{A})$ denotes the Hausdorff distance between $\mathcal{A}$ and $\mathcal{B}$ in the 2-norm.

II. Tube Model Predictive Control

This section reviews the main concepts of Tube MPC and introduces the notation used throughout the paper.

A. Uncertain Linear Systems

We consider uncertain discrete-time systems

$$x_{k+1} = A_k x_k + B_k u_k + w_k, \tag{1}$$

where $x_k \in \mathcal{X} \subseteq \mathbb{R}^{n_x}$ and $u_k \in \mathcal{U} \subseteq \mathbb{R}^{n_u}$ denote the state and input at time $k \in \mathbb{N}$. The sets $\mathcal{X}$ and $\mathcal{U}$ are closed and convex, and $w_k \in \mathcal{W}$ is an additive disturbance with $\mathcal{W}$ compact and convex.

The matrices A_k and B_k are uncertain and time-varying, but belong to a known polytopic set

$$\Delta := \mathrm{convh}\Big(\{(A^{(1)}, B^{(1)}),..., (A^{(\mathsf{m})}, B^{(\mathsf{m})})\}\Big).$$

B. Robust Control Tubes

Let $\mathcal{F}(X)$ denote the set of sets that can be reached from a given set $X \subseteq \mathbb{R}^{n_x}$; that is,

$$\mathcal{F}(X) := \left\{ X^+ \subseteq \mathbb{R}^{n_x} \;\middle|\; \begin{array}{l} \forall\, x \in X,\ \exists\, u \in \mathcal{U} : \\ \forall\, (A,B) \in \Delta,\ w \in \mathcal{W}, \\ Ax + Bu + w \in X^+ \end{array} \right\}.$$

A sequence of sets $X_0, X_1, \ldots \subseteq \mathcal{X}$ is called a feasible Robust Control Tube (RCT) if

$$\forall k \in \{0, \ldots, N-1\}, \quad X_{k+1} \in \mathcal{F}(X_k). \tag{2}$$

Moreover, a set $X \subseteq \mathcal{X}$ is called a feasible Robust Control Invariant (RCI) set if (X, X) is an RCT.

C. Optimization of RCTs

Conceptually, Tube MPC optimizes an RCT online so that the first set of the sequence contains the current state measurement. A typical optimal control formulation is

$$\begin{aligned} \min_{X_0,\ldots,X_N} \quad & L_0(X_0) + \sum_{k=0}^{N-1} L(X_k) + L_N(X_N) \\ \text{s.t.} \quad & \begin{cases} \forall k \in \{0,..., N-1\}, \\ X_{k+1} \in \mathcal{F}(X_k), \\ x \in X_0,\ X_k \subseteq \mathcal{X}. \end{cases} \end{aligned} \tag{3}$$

Here, x denote the current state, and L_0, L, L_N the initial, stage and terminal costs. Suitable choices for these functions that ensure closed-loop stability are detailed in [13]. Alternative formulations may also introduce penalties on control policies, which are hidden in the definition of $\mathcal{F}$; for an in-depth discussion, see [4].

III. Polytopic Tube MPC Schemes

Directly solving the set-based optimization problem in (3) is generally intractable due to its infinite-dimensional and non-convex nature. To address this, we adopt a convex reformulation based on polytopic set parameterization.

A. Configuration-Constrained Polytopes

Throughout this paper, we denote a polytope as

$$\mathcal{P}(y) := \{x \in \mathbb{R}^{n_x} \mid Fx \le y\}, \tag{4}$$

where $F \in \mathbb{R}^{\mathsf{f} \times n_x}$ is a fixed matrix and $y \in \mathbb{R}^{\mathsf{f}}$ is a parameter vector. We assume that $Fx \le 0$ implies $x = 0$, which guarantees that $\mathcal{P}(y)$ is bounded (and possibly empty) for any y. To preserve the polytope's combinatorial structure, we restrict y to a *configuration* cone

$$\mathcal{E} := \{y \in \mathbb{R}^{\mathsf{f}} \mid Ey \le 0\},$$

ensuring that the face structure of $\mathcal{P}(y)$ remains invariant for all $y \in \mathcal{E}$. Under this condition, there exists a set of matrices $V := \{V_j \mid j = 1,..., \mathsf{v}\}$ such that

$$\mathcal{P}(y) = \mathrm{convh}(\{V_j y \mid j = 1,..., \mathsf{v}\}), \quad \forall y \in \mathcal{E}. \tag{5}$$

Constructing such configuration triples (F, E, V) is non-trivial; one possible approach is described in [14, Sec. II.A]. The implications of fixing a configuration and methods for refining configuration triples will be discussed in the following sections.

B. Configuration-Constrained RCTs

The main advantage of configuration-constrained polytopes is their ability to parameterize a RCT using a single set of optimization variables for both facets and vertices. For a given configuration triple (F, E, V), we define the convex set

$$\mathbb{S} := \left\{ \begin{pmatrix} y \\ u \\ y^+ \end{pmatrix} \;\middle|\; \begin{array}{l} \forall\, (i,j) \in \{1,..., \mathsf{m}\} \times \{1,..., \mathsf{v}\}, \\ F(A^{(i)} V_j y + B^{(i)} u_j) + d \le y^+, \\ Ey \le 0,\ V_j y \in \mathcal{X},\ u_j \in \mathcal{U} \end{array} \right\}, \tag{6}$$

where $d_k := \max\{F_k w : w \in \mathcal{W}\}$ for all $k \in \{1,..., \mathsf{f}\}$ and $u_j \in \mathcal{U}$ denotes the control input at vertex j. Then, the following statement holds.

Proposition 1: Let $y_0, y_1, \ldots \in \mathcal{E}$ be a given sequence of parameters. Then $\mathcal{P}(y_0), \mathcal{P}(y_1), \ldots$ is a feasible RCT if and only if there exists a sequence of inputs $u_0, u_1, \ldots \in \mathbb{R}^{\mathsf{v} \cdot n_u}$ such that $(y_k, u_k, y_{k+1}) \in \mathbb{S}$ for all $k \in \mathbb{N}$.

Proof: The statement follows by combining the results from [11, Cor. 4] and [14, Prop. 1]. ■

Corollary 1: A polytope $\mathcal{P}(y)$ with $y \in \mathcal{E}$ is an RCI set if and only if there exists a $u \in \mathbb{R}^{\mathsf{v} \cdot n_u}$ such that $(y, u, y) \in \mathbb{S}$.

Proof: The result follows from Proposition 1 and the definition of RCI sets. ■

C. Optimal Configuration-Constrained RCIs

Corollary 1 can be used to compute an optimal configuration-constrained RCI polytope $\mathcal{P}(y_m)$. Given a convex stage cost $\ell(\cdot,\cdot)$, the parameter $y_m \in \mathcal{E}$ is a minimizer of the optimization problem

$$\begin{aligned} (y_m, u_m) \in \arg\min_{y,u}\ & \ell(y, u) \\ \text{s.t. }& (y, u, y) \in \mathbb{S}. \end{aligned} \tag{7}$$

If an explicit expression for the stage cost L in (3) such that $\ell(y, u) = L(\mathcal{P}(y))$ exists, then ℓ does not depend on u. In practice, however, it is common to define the objective by introducing suitable control penalties; for this reason, ℓ is often modeled as a strongly convex quadratic function, cf. [15, Sec. 2.D], so that the set of optimizers is a singleton.

D. Fully-parameterized CCTMPC for Tracking

One way to implement Tube MPC within the configuration-constrained framework is to compute a sequence of parameters $((y_0, u_0), (y_1, u_1), \cdots)$ that converges to the optimal RCI set parameters (y_m, u_m). A simple approach is to minimize the quadratic deviation from these optimal parameters. Specifically, we solve the strictly convex quadratic program

$$\begin{aligned} \min_{\mathbf{y},\mathbf{u}} \quad & \sum_{k=0}^{N-1} \left\| \begin{bmatrix} y_k - y_m \\ u_k - u_m \end{bmatrix} \right\|_Q^2 + \left\| \begin{bmatrix} y_N - y_m \\ u_N - u_m \end{bmatrix} \right\|_P^2 \\ \text{s.t.} \quad & \begin{cases} \forall k \in \{0, \ldots, N-1\}, \\ (y_k, u_k, y_{k+1}) \in \mathbb{S}, \\ Fx \le y_0, \\ (y_N, u_N, \gamma y_N + (1-\gamma) y_m) \in \mathbb{S}, \end{cases} \end{aligned} \tag{8}$$

where $\mathbf{y} = (y_0, ..., y_N)$ and $\mathbf{u} = (u_0, ..., u_N)$ stack the sequence of tube parameters and vertex control inputs, respectively. Here, $Q, P \succ 0$ are are weighting matrices in $\mathbb{R}^{(\mathsf{f}+\mathsf{v}\cdot n_u)\times(\mathsf{f}+\mathsf{v}\cdot n_u)}$, and $\gamma \in (0,1)$ is a user-defined parameter that helps ensure recursive feasibility and stability [15].

Problem (8) is parametric in the current state x. We denote its unique minimizers by $(\mathbf{y}^*(x), \mathbf{u}^*(x))$, and define the control law as

$$\mu_{\mathrm{c}}(x) := \arg\min_{u\in\mathcal{U}} \ u^\top u \quad \text{s.t.} \begin{cases} \forall i \in \{1, ..., \mathsf{m}\}, \\ F(A^{(i)}x + B^{(i)}u) + d \leq y_1^*(x). \end{cases} \tag{9}$$

By Proposition 1, feasibility of (9) is guaranteed whenever (8) is feasible, ensuring the existence of $(\mathbf{y}^*(x), \mathbf{u}^*(x))$. The closed-loop system then evolves as

$$\forall k \in \mathbb{N}, \qquad x_{k+1} = A_k x_k + B_k \mu_{\mathrm{c}}(x_k) + w_k. \tag{10}$$

From [15, Cor. 1], we recall the theoretical properties of the controller.

Proposition 2: Let $\gamma \in (0,1)$, and let $Q \succ 0$ and $P \succ 0$ satisfy $Q + \gamma^2 P \preceq P$. Then, for all uncertainty realizations $(A_k, B_k) \in \Delta$ and disturbances $w_k \in \mathcal{W}$, the following statements hold for all $k \in \mathbb{N}$:

1) If Problem (8) is feasible with $x = x_0$, then it remains feasible for all subsequent states x_k of (10).
2) Define
$$\mathcal{L}(\mathbf{y}, \mathbf{u}) := \sum_{k=0}^{N-1} \left\| \begin{bmatrix} y_k - y_m \\ u_k - u_m \end{bmatrix} \right\|_Q^2 + \left\| \begin{bmatrix} y_N - y_m \\ u_N - u_m \end{bmatrix} \right\|_P^2.$$
Then, the Lyapunov inequality
$$\mathcal{L}(\mathbf{y}^*(x_{k+1}), \mathbf{u}^*(x_{k+1})) \leq \mathcal{L}(\mathbf{y}^*(x_k), \mathbf{u}^*(x_k))$$
holds, with $\mathcal{L}(\mathbf{y}, \mathbf{u}) = 0$ only at $x_k \in \mathcal{P}(y_m)$, and
$$\lim_{k\to\infty} (\mathbf{y}^*(x_k), \mathbf{u}^*(x_k)) = ((y_m, ..., y_m), (u_m, ..., u_m)).$$
3) The distance between the state in (10) and the optimal RCI set converges to 0; that is, $\lim_{k\to\infty} x_k \in \mathcal{P}(y_m)$.

Proof: The proof follows by applying [15, Cor. 1] to the case of fixed optimal RCI set parameters. ∎

While Proposition 2 establishes strong theoretical properties for (8), its online solution can be computationally demanding. For instance, if $\mathcal{X}$ and $\mathcal{U}$ are polyhedra defined by $m_{\mathcal{X}}$ and $m_{\mathcal{U}}$ half-spaces, respectively, and $m_{\mathcal{E}}$ is the number of rows in E, then Problem (8) involves $(N+1)\times(\mathsf{f}+\mathsf{v}\cdot n_u)$ decision variables and $(N+1)\times(\mathsf{fmv}+m_{\mathcal{E}}+\mathsf{v}(m_{\mathcal{X}}+m_{\mathcal{U}}))$ constraints.

E. Homothetic CCTMPC for Tracking

One way to reduce the number of optimization variables in the above Tube MPC formulation is to work with a homothetic transformation of a given polytope, denoted by $\mathcal{P}(y_m)$. To formalize this, we introduce the following standard assumption (see also [7]).

Assumption 1: The optimal RCI set satisfies the condition $(0,0) \in \mathcal{P}(y_m) \times \mathrm{convh}(\{u_{m,j} \in \mathcal{U} \mid j \in \{1, ..., \mathsf{v}\}\})$.

Following [7], we introduce a scaling factor $\alpha \in \mathbb{R}$ and offset vectors $(z, v) \in \mathbb{R}^{n_x+n_u}$, such that

$$y = \alpha y_m + Fz, \quad u_j = \alpha u_{m,j} + v, \ j \in \{1, ..., \mathsf{v}\}. \tag{11}$$

From [11], the construction of the matrix E and the associated configuration cone $\mathcal{E}$ implies

$$y_m \in \mathcal{E} \ \Rightarrow \ \alpha y_m + Fz \in \mathcal{E}, \quad \forall \alpha \geq 0, \ z \in \mathbb{R}^{n_x}. \tag{12}$$

Thus, $\mathcal{P}(\alpha y_m + Fz)$ is a configuration-constrained polytope for all $\alpha \geq 0$.

We assume that the constraint sets are polytopes $\mathcal{X} := \{x \in \mathbb{R}^{n_x} \mid H^x x \leq h^x\}$ and $\mathcal{U} := \{u \in \mathbb{R}^{n_u} \mid H^u u \leq h^u\}$. Then, we define for all $j \in \{1, ..., \mathsf{v}\}$

$$h_m^x := \max_j H^x V_j y_m, \quad h_m^u := \max_j H^u u_{m,j},$$

with the maximum taken row-wise. Then, the inclusions $V_j(\alpha y_m + Fz) \in \mathcal{X}$ and $\alpha u_{m,j} + v \in \mathcal{U}$ hold for all the vertices if and only if

$$\begin{bmatrix} H^x & 0 \\ 0 & H^u \end{bmatrix} \begin{bmatrix} z \\ v \end{bmatrix} + \begin{bmatrix} h_m^x \\ h_m^u \end{bmatrix} \alpha \leq \begin{bmatrix} h^x \\ h^u \end{bmatrix}. \tag{13}$$

Finally, we define the set $\bar{\mathbb{S}} \subseteq \mathbb{R}^{2n_x+n_u+2}$ as

$$\bar{\mathbb{S}} := \left\{ \begin{pmatrix} (z, \alpha) \\ v \\ (z^+, \alpha^+) \end{pmatrix} \middle| \begin{array}{l} \alpha \geq 0, \quad (13), \quad \forall i \in \{1, ..., \mathsf{m}\}, \\ F(A^{(i)}z + B^{(i)}v) + (1-\alpha)d \\ \qquad + \alpha y_m \leq \alpha^+ y_m + Fz^+, \end{array} \right\}.$$

Corollary 2: Let $(z_k, \alpha_k)_{k\in\mathbb{N}}$ be such that for all $k \in \mathbb{N}$ there exist inputs v_k satisfying $((z_k, \alpha_k), v_k, (z_{k+1}, \alpha_{k+1})) \in \bar{\mathbb{S}}$. Then, the sequence $(\mathcal{P}(\alpha_k y_m + Fz_k))_{k\in\mathbb{N}}$ is an RCT.

Proof: The state, input, and configuration constraints for the RCT follow from (13) and (12). Substituting the parameterization in (11) into the set $\mathbb{S}$ and applying Proposition 1, along with the observation that (y_m, u_m) satisfy $F(A^{(i)}V_j y_m + B^{(i)}u_{m,j}) + d \leq y_m$ for all $(i,j) \in \{1, ..., \mathsf{m}\} \times \{1, ..., \mathsf{v}\}$, completes the proof. ∎

By exploiting Corollary 2, we formulate our Homothetic TMPC scheme based on the parametric QP

$$\begin{aligned} \min_{\mathbf{z},\boldsymbol{\alpha},\mathbf{v}} \ & \sum_{k=0}^{N-1} \left\| \begin{bmatrix} z_k \\ v_k \\ \alpha_k - 1 \end{bmatrix} \right\|_{\bar{Q}}^2 + \left\| \begin{bmatrix} z_N \\ v_N \\ \alpha_N - 1 \end{bmatrix} \right\|_{\bar{P}}^2 \\ \text{s.t.} \ & \begin{cases} \forall k \in \{0, \ldots, N-1\}, \\ ((z_k, \alpha_k), v_k, (z_{k+1}, \alpha_{k+1})) \in \bar{\mathbb{S}} \\ Fx \leq \alpha_0 y_m + Fz_0, \\ ((z_N, \alpha_N), v_N, (\gamma z_N, \gamma\alpha_N + 1 - \gamma)) \in \bar{\mathbb{S}}. \end{cases} \end{aligned} \tag{14}$$

Here, $\mathbf{z} = (z_0, ..., z_N)$, $\boldsymbol{\alpha} = (\alpha_0, ..., \alpha_N)$, and $\mathbf{v} = (v_0, ..., v_N)$ stack the sequence of homothetic tube parameters, and the weighting matrices $\bar{Q}, \bar{P} \succ 0$ are in $\mathbb{R}^{(n_x+n_u+1)\times(n_x+n_u+1)}$. We denote the optimizers of (14) as $(\mathbf{z}^*(x), \boldsymbol{\alpha}^*(x), \mathbf{v}^*(x))$, and define the control law as

$$\mu_{\mathrm{h}}(x) := \arg\min_{u\in\mathcal{U}} \ u^\top u \quad \text{s.t.} \begin{cases} \forall i \in \{1, ..., \mathsf{m}\}, \\ F(A^{(i)}x + B^{(i)}u) + d \\ \qquad \leq \alpha_1^*(x) y_m + Fz_1^*(x). \end{cases} \tag{15}$$

Finally, the closed-loop system evolves as

$$x_{k+1} = A_k x_k + B_k \mu_{\rm h}(x_k) + w_k. \tag{16}$$

Corollary 3: Let $\gamma \in (0,1)$, and let $\bar{Q} \succ 0$ and $\bar{P} \succ 0$ satisfy $\bar{Q} + \gamma^2 \bar{P} \preceq \bar{P}$. Then, the closed-loop system under (15) satisfies the same properties as in Proposition 2.

Proof: Define the matrix $\tilde{\mathbb{I}} = \mathbf{1}_{\mathsf{v}} \otimes \mathbb{I}_{n_u}$ and

$$\tilde{F} := \begin{bmatrix} F & 0 & y_m \\ 0 & \tilde{\mathbb{I}} & u_m \end{bmatrix} \in \mathbb{R}^{(\mathsf{f}+\mathsf{v}\cdot n_u)\times(n_x+n_u+1)}. \tag{17}$$

can then be written as Problem (8) with optimization variables $(\mathbf{z}, \boldsymbol{\alpha}, \mathbf{v})$, additional linear equalities $y_k = \alpha_k y_m + F z_k$ and $u_k = \alpha_k u_m + \tilde{\mathbb{I}}\, v_k$ and cost matrices given by $Q = \|\tilde{F}^\dagger\|_{\bar{Q}}^2$ and $P = \|\tilde{F}^\dagger\|_{\bar{P}}^2$, where $\tilde{F}^\dagger$ is well-defined since $\tilde{F}$ is full column rank. Recursive feasibility follows from the convexity of $\bar{\mathbb{S}}$ and these equalities. Lyapunov stability follows because Q and P are positive definite on the nullspace of the equality constraints, and the inequality $\bar{Q} + \gamma^2 \bar{P} \preceq \bar{P}$ implies $Q + \gamma^2 P \preceq P$. ■

We remark that Problem (14) is computationally less demanding to solve online than Problem (8), since it has $(N+1) \times (n_x + n_u + 1)$ optimization variables and $(N+1) \times (\mathsf{f}\mathsf{m} + 1 + m_{\mathcal{X}} + m_{\mathcal{U}})$ constraints.

F. A family of CCTMPC schemes

The formulations (8) and (14) represent two extremes in the use of configuration-constrained polytopes for TMPC synthesis. Specifically, (14) relies on a restricted parameterization of (y, u) in terms of (y_m, u_m) via (11), whereas more flexible formulations of CCTMPC can be derived by relaxing this structure. These intermediate schemes aim to balance computational efficiency and control conservatism in practical applications.

To illustrate this flexibility, we propose two intermediate schemes. For both formulations, admissible control sets—constructed following the structure of $\mathbb{S}$—can be systematically derived by substituting the proposed (y, u)-parameterizations into the synthesis framework. In addition, the inherent inclusion $(y_m, u_m, y_m) \in \mathbb{S}$ is explicitly leveraged to ensure recursive feasibility.

1) Partially-parameterized CCTMPC: In this scheme, a subset of the vertices of $\mathcal{P}(y)$ is parameterized as homothetic transformations of the corresponding vertices of $\mathcal{P}(y_m)$, while the remaining ones are freely optimized. Let $J_{\rm p} \subseteq \{1,...,\mathsf{v}\}$ denote the indices of the vertices to be parameterized as

$$V_j y = \alpha V_j y_m + z, \quad \forall j \in J_{\rm p}. \tag{18}$$

For each j, let $i(j) \subset \{1,...,\mathsf{f}\}$ denote the set of indices of the halfspaces intersecting at the vertex $V_j y$. To achieve (18), define the index set $I_{\rm p} := \cup_{j \in J_{\rm p}} i(j)$ and the matrix

$$S_{\rm p} = \sum_{i \in I_{\rm p}} e_i e_i^\top.$$

where e_i is the i-th column of the identity matrix $\mathbb{I}_{\mathsf{f}}$. Finally, let $I_{\rm f} := \{1,...,\mathsf{f}\} \setminus I_{\rm p}$. Then, the polytope $\mathcal{P}(\alpha S_{\rm p} y_m + Fz + S_{\rm f} \hat{y})$ satisfies (18) if $\alpha S_{\rm p} y_m + Fz + S_{\rm f} \hat{y} \in \mathcal{E}$. For consistency, the vertex inputs for $j \in J_{\rm p}$ are parameterized as $u_j = \alpha u_{m,j} + v$, while the inputs corresponding to the remaining vertices are freely optimized.

Denoting the cardinality of $J_{\rm p}$ and $I_{\rm f}$ as $\hat{\mathsf{v}}$ and $\hat{\mathsf{f}}$ respectively, the resulting Partially-parameterized CCTMPC scheme involves $(N+1) \times (\hat{\mathsf{f}} + n_x + n_u + 1 + (\mathsf{v} - \hat{\mathsf{v}}) n_u)$ decision variables, with $\hat{\mathsf{v}} > 0$. Note that if $\hat{\mathsf{v}} = \mathsf{v}$, then $\hat{\mathsf{f}} = 0$ by construction and the scheme reduces to the Homothetic CCTMPC one. Conversely, for $\hat{\mathsf{v}} = 0$, it coincides with the Fully-parameterized formulation. The number of linear inequality constraints equals that of the fully parameterized scheme for any $\hat{\mathsf{v}} \in \{0,...,\mathsf{v}-1\}$, and reduces to that of Homothetic CCTMPC when $\hat{\mathsf{v}} = \mathsf{v}$.

The selection of $J_{\rm p}$ should ensure that the stabilizable region encompasses the desired set of initial states. Developing systematic methods for choosing $J_{\rm p}$ based on this requirement remains an open direction for future research.

2) Homothetic CCTMPC with optimized controls: Inspired by [10], this variant parameterizes $y = \alpha y_m + Fz$, while all vertex control inputs are freely optimized. This results in $(N+1) \times (n_x + 1 + \mathsf{v} \cdot n_u)$ decision variables and $(N+1) \times (\mathsf{f}\mathsf{m}\mathsf{v} + 1 + m_{\mathcal{X}} + \mathsf{v} m_{\mathcal{U}})$ linear inequality constraints. Its stabilizable region lies between that of Homothetic CCTMPC and the fully parameterized scheme.

IV. COMPUTING TEMPLATE POLYTOPES

This section introduces a computational procedure for constructing configuration triples for TMPC synthesis. The approach iteratively refines the triple (F, E, V) so that, at each iteration, the feasibility set $\mathbb{S}$ (or $\bar{\mathbb{S}}$) remains nonempty, the number of polytope vertices increases by a fixed amount, and the size of the resulting RCI set increases.

A. Iterative Refinement of the Configuration Triple

Suppose a configuration triple (F, E, V) is given such that $\mathbb{S}$ is nonempty. Let $\mathcal{X} = \mathrm{convh}(\{\xi_1, ..., \xi_{\rm s}\})$, and consider the optimization problem

$$\sigma := \min_{y_M \geq 0, u, z} \sum_{i=1}^{\rm s} \|\xi_i - z_i\|_2^2 \tag{19}$$
$$\text{s.t.} \quad (y_M, u, y_M) \in \mathbb{S}, \; F z_i \leq y_M, \; i \in \{1, ..., {\rm s}\}.$$

Although dependencies are omitted for brevity, this problem is parametric in the configuration triple. Let $(y_M^\star, u^\star, z^\star)$ be an optimizer of (19). Then, the RCI polytope $\{x \in \mathcal{X} \mid Fx \leq y_M^\star\}$ contains points $z_1^\star, \ldots, z_{\rm s}^\star$ that minimize the aggregated distance to the vertices of $\mathcal{X}$.

Algorithm 1 iteratively refines the configuration triple by adding facets to F while ensuring that σ is nonincreasing. The core operations occur in the inner (parallelizable) loop, Steps 6–9. For each vertex c_j, a supporting hyperplane $\{x \mid c_j^\top x \leq \zeta\}$ is computed (Step 6), and then scaled by κ so that only c_j is excluded from the polytope $\{x \mid Fx \leq y^i, \; c_j^\top x \leq \kappa\zeta\}$ (Step 7). A new configuration triple for this polytope is then computed (Step 8), and the candidate yielding the largest RCI set is selected (Steps 9–11). In

Algorithm 1: Configuration Triple Refinement

Data: Initial triple (F, E, V), $i_{\max} \geq 1$

1 Set $i \leftarrow 1$;
2 Solve (19) with (F, E, V), set $\sigma^i \leftarrow \sigma$, $y^1 \leftarrow y_M^\star$;
3 **while** $i \leq i_{\max}$ **do**
4   Set $c_j \leftarrow V_j y^i$ for $j \in \{1,...,\mathsf{v}\}$;
5   **parfor** $j \leftarrow 1$ **to** v **do**
6         $\zeta \leftarrow \max_z \, c_j^\top z$ s.t. $Fz \leq y^i$;
7   Set $\kappa \in (0, 1)$ such that $c_j^\top c_k < \kappa\zeta, \quad \forall k \in \{1,...,\mathsf{v}\} \setminus \{j\}$;
8   Construct new triple (F^j, E^j, V^j) for the polytope $\{x \,|\, Fx \leq y^i,\, c_j^\top x \leq \kappa\zeta\}$;
9   Solve (19) with (F^j, E^j, V^j), set $\overline{\sigma}^j \leftarrow \sigma$ and $\overline{y}^j \leftarrow y_M^\star$;
10   Select $j^\star$ such that $\overline{\sigma}^{j^\star} \leq \overline{\sigma}^j \; \forall j \in \{1,...,\mathsf{v}\}$;
11   Update $(F, E, V) \leftarrow (F^{j^\star}, E^{j^\star}, V^{j^\star})$;
12   Set $i \leftarrow i + 1$, $\sigma^i \leftarrow \overline{\sigma}^{j^\star}$, and $y^i \leftarrow \overline{y}^{j^\star}$;
13 **return** (F, E, V).

practice, Step 4 should remove redundant vertices before enumeration to ensure that the loop operates only on unique vertices.

Proposition 3: The sequence $(\sigma^1, ..., \sigma^{i_{\max}})$ generated by Algorithm 1 is nonincreasing.

Proof: Let i be an arbitrary iteration and (y_M, u, z) a minimizer of (19) with optimal value σ^i. For any vertex index, Step 9 ensures that z remains feasible with $\left((y_M^\top, \zeta)^\top\right)$, and u is chosen so that new vertex inputs coincide with u_j. Since the added halfspace is redundant (Step 6), $\overline{\sigma}^j \leq \sigma^i$. By Steps 10 and 12, $\sigma^{i+1} \leq \overline{\sigma}^j$ for all $j \in \{1,...,\mathsf{v}\}$, proving monotonicity. ∎

Remark 1: Algorithm 1 applies to both simple and non-simple polytopes. When truncating a non-simple vertex, the operation introduces new simple vertices equal in number to the degree of the cut vertex. Repeated truncations eventually yield a simple polytope, consistent with the density of simple polytopes in the parameter space [14, Prop. 1].

Remark 2: For simple polytopes, the number of rows in E is bounded by the number of edges [4, Sec. 2.14]. Moreover, truncations of faces up to dimension $n_x - 2$ preserve simplicity [16], enabling partial reuse of matrices E and V from previous iterations. These properties significantly reduce the computational cost of Step 8 and provide insights for more efficient truncation strategies.

B. Computing Initial Matrix F

To initialize Algorithm 1, we compute a feasible configuration triple (F, E, V) using a nonlinear programming (NLP) approach inspired by [17], [18]. Given a polytope

$$\{x \in \mathbb{R}^{n_x} \mid Fx \leq 1\} = \operatorname{convh}(\{V_1 1, ..., V_\mathsf{v} 1\}),$$

the procedure computes an invertible matrix $T \in \mathbb{R}^{n_x \times n_x}$ such that $\{x \in \mathbb{R}^{n_x} \mid FT^{-1}x \leq 1\}$ is an RCI polytope with vertices $\{TV_1 1, \ldots, TV_\mathsf{v} 1\}$.

This NLP is formulated as

$$\min_{T,u,\varepsilon} \quad \varepsilon^\top \varepsilon$$
$$\text{s.t.} \begin{cases} \forall (i,j,k) \in \{1,...,\mathsf{m}\} \times \{1,...,\mathsf{v}\} \times \{1,...,\mathsf{w}\}, \\ FT^{-1}(A^{(i)}TV_j 1 + B^{(i)}u_j + w_k) \leq 1, \\ TV_j 1 \in \mathcal{X}, \; u_j \in \mathcal{U}, \\ \mathcal{X} \subseteq \{x \mid FT^{-1}x \leq 1 + \varepsilon\}. \end{cases} \tag{20}$$

where $\{w_1, \ldots, w_\mathsf{w}\}$ are the vertices of $\mathcal{W}$.

The inclusion $\mathcal{X} \subseteq \{x \mid FT^{-1}x \leq 1 + \varepsilon\}$ in (20) can be expressed via duality as

$$\Lambda h^x \leq 1 + \varepsilon, \;\; \Lambda H^x = FT^{-1}, \;\; \Lambda \geq 0,$$

with $\Lambda \in \mathbb{R}^{\mathsf{f} \times \mathsf{w}}$ being an additional optimization variable.

Since T defines an invertible linear transformation, the face configuration—and thus the configuration cone $\mathcal{E}$—is preserved (see [19, Sec. 2.6], [20, Sec. 1.1]).

V. Numerical Examples

We validate our procedural construction through two numerical examples[1]. In both cases, the base polytope for (20) is chosen as an n_x-simplex with $F = [-\mathbb{I}_{n_x} \; \mathbf{1}]^\top$, ensuring the origin lies in its interior for any positive offset vector. The terminal set parameter γ is set to 0.95. We denote the stabilizable region of the fully-parameterized CCTMPC scheme with horizon N as $\mathcal{O}_\mathrm{c}(N)$, and that of the Homothetic CCTMPC (HTMPC) scheme as $\mathcal{O}_\mathrm{h}(N)$. Computational times for Problems (8) and (14) were recorded on an Intel Core i5-8350U CPU running Ubuntu 24.04.

A. Illustrative Example

We consider a discretized triple integrator subject to both additive and multiplicative uncertainties. The system matrices belong to the polytopic uncertainty set

$$\Delta := \operatorname{convh}\left(\{(\alpha_i \bar{A}, \alpha_i \bar{B}) \mid \alpha_i \in \{0.9, 1.1\}\}\right),$$

where the nominal matrices are

$$\bar{A} = \begin{bmatrix} 1 & h & h^2/2 \\ 0 & 1 & h \\ 0 & 0 & 1 \end{bmatrix}, \quad \bar{B} = \begin{bmatrix} h^3/6 \\ h^2/2 \\ h \end{bmatrix},$$

with $h = 1/4$. The additive disturbance set is

$$\mathcal{W} = \left\{ \begin{bmatrix} h & h^2/2 & h^3/6 \\ 1 & h & h^2/2 \\ 0 & 1 & h \end{bmatrix} w \;\middle|\; w \in \tfrac{1}{20}[-1,\, 1]^3 \right\},$$

and the state and input constraints are $\mathcal{X} = [-5,\, 5]^3$ and $\mathcal{U} = [-3,\, 3]$, respectively. The initial template obtained from Problem (20) is

$$FT^{-1} = \begin{bmatrix} 1.1856 & 2.1991 & 0.2544 \\ 0 & 1.4770 & 1.7581 \\ -2.6514 & -5.3810 & -2.6623 \\ 1.4658 & 1.7048 & 0.6498 \end{bmatrix}.$$

[1]MATLAB code available at `https://github.com/fil-bad/EfficientCCTMPC`

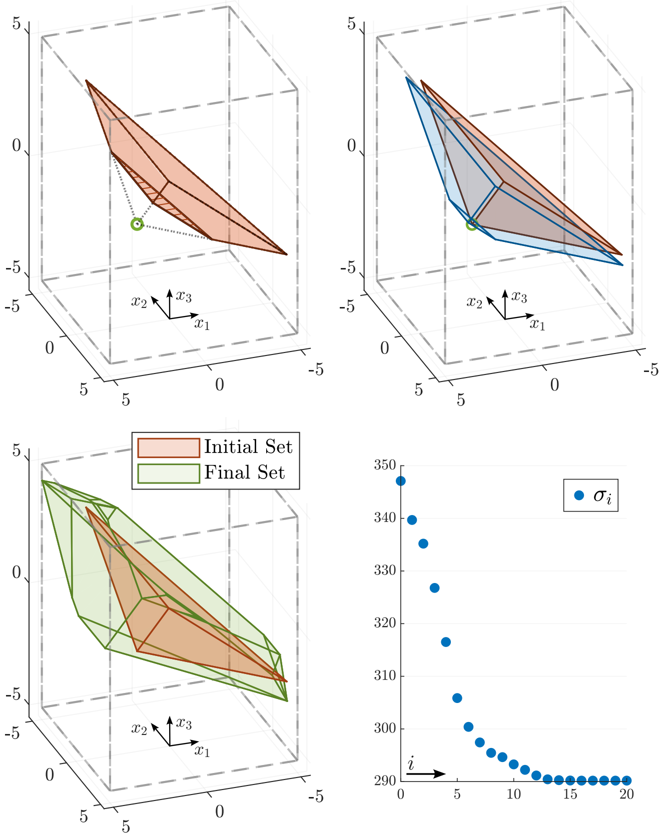

Fig. 1. Steps of Algorithm 1: `Top-left`: First iteration—selected vertex i^* (green) marked for cutting; shaded facet indicates the cut at $\kappa\zeta$. `Top-right`: CC-RCI set (blue) after one iteration. `Bottom-left`: CC-RCI set before (red) and after $i_{\max}$ iterations (green). `Bottom-right`: Evolution of σ^i versus iteration index i.

Algorithm 1 is executed for $i_{\max} = 20$ iterations, exploring polytopes with $\mathsf{f} = n_x+1+i$ facets and $\mathsf{v} = n_x+1+i(n_x-1)$ vertices, for $i \in [1, i_{\max}]$. Figure 1 illustrates the iterative refinement process.

To implement the control schemes, we select the template from iteration $i = 10$. The optimal RCI cost in (7) is

$$\ell(y,u) = \sum_{j=1}^{\mathsf{v}} \left\| \begin{bmatrix} (\bar{V}-V_j)y \\ (\bar{U}-U_j)u \end{bmatrix} \right\|^2_{Q_v} + \left\| \begin{bmatrix} \bar{V} & 0 \\ 0 & \bar{U} \end{bmatrix} \begin{bmatrix} y \\ u \end{bmatrix} \right\|^2_{Q_c},$$

with $\bar{V} = \sum_{j=1}^{\mathsf{v}} V_j$, $\bar{U} = \sum_{j=1}^{\mathsf{v}} U_j$, $Q_v = 10^{-1}\mathbb{I}_4$, and $Q_c = \mathbb{I}_4$. The tracking cost matrices are $Q = \mathbb{I}_{38}$ and $P = (1-\gamma^2)^{-1}Q$ for CCTMPC, and adapted as in (17) for HTMPC. The prediction horizon is $N = 3$.

Figure 2 compares $\mathcal{O}_{\mathrm{c}}(3)$ and $\mathcal{O}_{\mathrm{h}}(3)$, and shows sampled trajectories converging to the optimal RCI set. Denoting $\mathcal{X}^-$ as the 6-step backward reachable set[2] from $\mathcal{X}$, the Hausdorff distances are $\mathrm{d}_{\mathcal{X}^-}(\mathcal{O}_{\mathrm{c}}(3)) = 3.3925$ and $\mathrm{d}_{\mathcal{X}^-}(\mathcal{O}_{\mathrm{h}}(3)) = 5.8220$ indicating that CCTMPC is less conservative than HTMPC. Computation times of $(\min, \mathrm{avg}, \max) = (2.59, 15.06, 76.96)$ [ms] for CCTMPC and $(1.04, 1.30, 3.67)$ [ms] for HTMPC using DAQP [21]

[2]The backward iteration procedure to compute the maximal RCI set ran out of memory after 6 steps.

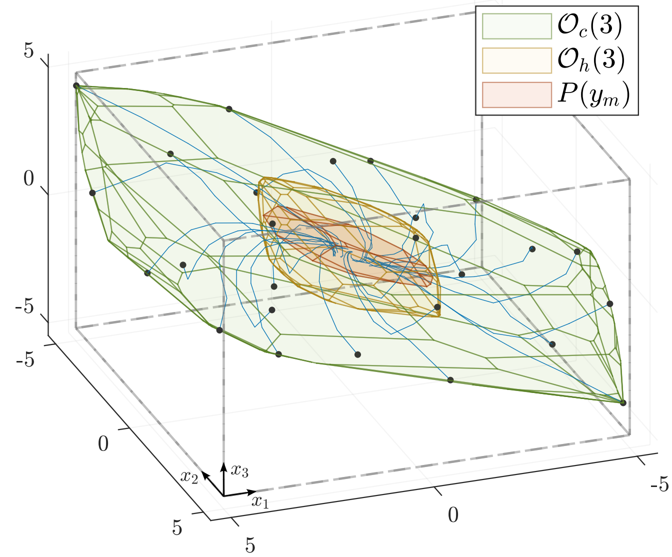

Fig. 2. Comparison of feasible regions for CCTMPC (green) and HTMPC (yellow) parameterizations. Sampled trajectories (blue) for CCTMPC converge to the optimal RCI set (red).

highlights the trade-off between increased flexibility and computational cost—a discrepancy that grows with template complexity.

B. Quadrotor System

We consider a 10-state quadrotor model as in [22], discretized with a timestep of 0.1 s and linearized at $x_{eq} = 0$ and $u_{eq} = [0, 0, k_T^{-1}g]^\top$, where $k_T = 0.91$ and g is the gravitational constant. State constraints are given by $\mathcal{X} = \{x \in \pm[4, 4, 2, 10, 10, 5, \pi/3, \pi/3, \pi, \pi]\}$, while the inputs constraints are $\mathcal{U} = \{(u_1, u_2) \in \pm[\pi/4]^2, u_3 \in [0, 2g] - (k_T^{-1}g)\}$. The additive disturbance set is $\mathcal{W} = \{B_w w \mid w \in \pm[0.05, 0.05, 0.1]\}$, with $B_w = [\mathbb{I}_3 \ \mathbf{0}_{3\times 7}]^\top$.

To illustrate the benefits of homothetic parameterization for high-dimensional systems, we first compute a template matrix F by solving (20), then enrich it by introducing a cutting plane at each vertex. This yields a polytope with $\mathsf{f} = 22$ facets and $\mathsf{v} = 110$ vertices. Although Algorithm 1 could systematically refine the template, we observed that $\sigma^i = \sigma^1$ for all $i > 1$, indicating convergence to a local minimum. Strategies to escape such minima (e.g., introducing arbitrary cuts instead of following Step 10) are under investigation.

Optimal RCI cost is computed using $\ell(y,u) = \|y\|_2^2 + \|u\|_2^2$, while the tracking cost matrices are $\bar{Q} = \mathbb{I}_{14}$, $\bar{P} = (1-\gamma^2)^{-1}\bar{Q}$ for HTMPC and $Q = \mathbb{I}_{352}$, $P = (1-\gamma^2)^{-1}Q$ for CCTMPC. Figure 3 compares the Hausdorff distance for HTMPC, $\mathrm{d}_{\mathcal{X}}(\mathcal{O}_{\mathrm{h}}(N))$ across different prediction horizons N, against CCTMPC with $N = 3$. For any $N \geq 5$, we obtain $\mathrm{d}_{\mathcal{X}}(\mathcal{O}_{\mathrm{h}}(N)) < \mathrm{d}_{\mathcal{X}}(\mathcal{O}_{\mathrm{c}}(3))$. In the same figure, the average computational time for CCTMPC(3) (334 [ms]) is compared against HTMPC(N) using Gurobi [23]: the runtime advantage of HTMPC is evident, not being influenced by the chosen template complexity.

Motivated by these results, we design an HTMPC controller using a template matrix FT^{-1} obtained by solving

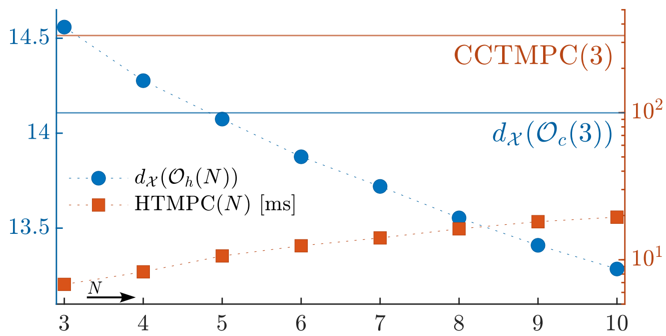

Fig. 3. Performance comparison of HTMPC for different prediction horizons N versus a CCTMPC(3): Hausdorff distance to state constraints (blue) and average computational time (red).

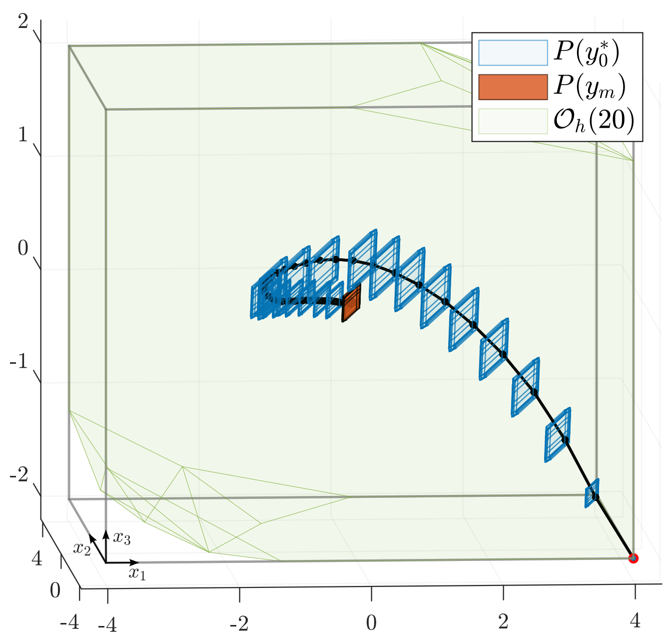

Fig. 4. Closed-loop evolution of HTMPC projected onto spatial coordinates. The red dot marks the initial state.

Problem (20) with $F = [\mathbb{I}_{10} - \mathbb{I}_{10}]^\top$, resulting in $\mathrm{v} = 1024$. Figure 4 shows closed-loop trajectories under Problem (14) with $N = 20$, where the tube $\mathcal{P}(\alpha_0 y_m + F z_0)$ converges to the optimal RCI set. Using this template, we report that $\mathrm{d}_{\mathcal{X}}(\mathcal{O}_{\mathrm{h}}(20)) = 10.355$, and Problem (14) requires an average of 22.9 [ms] per iteration.

VI. Conclusions

This paper advances the CCTMPC framework by: (i) introducing a family of RCT parameterizations and control schemes that enable systematic trade-offs between computational complexity and conservatism; (ii) proposing an algorithm for generating configuration-constrained triples of user-specified complexity. The effectiveness of these contributions was demonstrated through numerical examples, including a 10-state quadrotor benchmark, highlighting the potential of CCTMPC for robust control of high-dimensional systems. Future work will focus on refining Algorithm 1 and developing efficient software tools for template synthesis exploiting configuration constraints.

References

[1] B. Houska and M. E. Villanueva, "Robust optimization for MPC," in *Handbook of Model Predictive Control*, S. Raković and W. Levine, Eds. Birkäuser, Cham, 2019, pp. 413–443.
[2] B. Kouvaritakis and M. Cannon, *Model Predictive Control: Classical, Robust and Stochastic*. Springer, 2015.
[3] J. B. Rawlings, D. Q. Mayne, and M. M. Diehl, *Model Predictive Control: Theory and Design*. Madison, WI: Nob Hill Publishing, 2015.
[4] B. Houska, M. A. Müller, and M. E. Villanueva, "Polyhedral control design: Theory and methods," *Annu Rev Control*, vol. 60, p. 100992, 2025.
[5] D. Q. Mayne, M. M. Seron, and S. V. Raković, "Robust model predictive control of constrained linear systems with bounded disturbances," *Automatica*, vol. 41, no. 2, pp. 219–224, 2005.
[6] S. V. Raković, "The implicit rigid tube model predictive control," *Automatica*, vol. 157, p. 111234, 2023.
[7] S. V. Raković, B. Kouvaritakis, R. Findeisen, and M. Cannon, "Homothetic tube model predictive control," *Automatica*, vol. 48, no. 8, pp. 1631–1638, 2012.
[8] S. V. Raković, W. S. Levine, and B. Açikmese, "Elastic tube model predictive control," in *Am. Control Conf. (ACC)*, 2016, pp. 3594–3599.
[9] J. Fleming, B. Kouvaritakis, and M. Cannon, "Robust Tube MPC for Linear Systems With Multiplicative Uncertainty," *IEEE Trans. Autom. Control*, vol. 60, no. 4, pp. 1087–1092, 2015.
[10] W. Langson, I. Chryssochoos, S. V. Raković, and D. Q. Mayne, "Robust model predictive control using tubes," *Automatica*, vol. 40, no. 1, pp. 125–133, 2004.
[11] M. E. Villanueva, M. A. Müller, and B. Houska, "Configuration-Constrained Tube MPC," *Automatica*, vol. 163, p. 111543, 2024.
[12] P.-O. Gutman and M. Cwikel, "Admissible sets and feedback control for discrete-time linear dynamical systems with bounded controls and states," *IEEE Trans. Autom. Control*, vol. 31, no. 4, pp. 373–376, 1986.
[13] M. E. Villanueva, E. De Lazzari, M. A. Müller, and B. Houska, "A set-theoretic generalization of dissipativity with applications in Tube MPC," *Automatica*, vol. 122, no. 109179, 2020.
[14] B. Houska, M. A. Müller, and M. E. Villanueva, "On Stabilizing Terminal Costs and Regions for Configuration-Constrained Tube MPC," *IEEE Control Syst. Lett.*, vol. 8, pp. 1961–1966, 2024.
[15] F. Badalamenti, S. K. Mulagaleti, A. Bemporad, B. Houska, and M. E. Villanueva, "Configuration-Constrained Tube MPC for Tracking," *IEEE Control Syst. Lett.*, 2024.
[16] V. M. Buchstaber and N. Y. Erokhovets, "Truncations of simple polytopes and applications," *Proc. Steklov Inst. Math.*, vol. 289, no. 1, pp. 104–133, 2015.
[17] S. K. Mulagaleti, M. Mejari, and A. Bemporad, "Parameter-Dependent Robust Control Invariant Sets for LPV Systems with Bounded Parameter-Variation Rate," *IEEE Trans. Autom. Control*, 2024.
[18] A. Gupta, H. Köroğlu, and P. Falcone, "Computation of robust control invariant sets with predefined complexity for uncertain systems," *Int. J. Robust Nonlinear Control*, vol. 31, no. 5, p. 1674–1688, 2020.
[19] G. M. Ziegler, *Lectures on Polytopes*, ser. Graduate texts in mathematics. New York, NY: Springer, 2008.
[20] B. Grunbaum and G. M. Ziegler, *Convex Polytopes*, 2nd ed., ser. Graduate texts in mathematics. New York, NY: Springer, 2003.
[21] D. Arnström, A. Bemporad, and D. Axehill, "A dual active-set solver for embedded quadratic programming using recursive LDL^T updates," *IEEE Trans. Autom. Control*, vol. 67, no. 8, pp. 4362–4369, 2022.
[22] H. Hu, X. Feng, R. Quirynen, M. E. Villanueva, and B. Houska, "Real-Time Tube MPC Applied to a 10-State Quadrotor Model," in *Am. Control Conf. (ACC)*, 2018, pp. 3135–3140.
[23] Gurobi Optimization, LLC, "Gurobi Optimizer Reference Manual," 2024.